Use of a hybrid method of Computational Aeroacoustics: the ducted diaphragm at low Mach number

Hybride Berechnungsmethode für Aeroakustik: Diaphragma in einem Rohr bei niedriger Machzahl

M. Piellard[1], C. Bailly[2]

[1] *Delphi Thermal, Luxembourg, Email: melanie.piellard@delphi.com*

[2] *LMFA – UMR CNRS 5509, Ecole Centrale de Lyon & IUF, France, E-mail : christophe.bailly@ec-lyon.fr*

Abstract

A hybrid method of aeroacoustic noise computation based on Lighthill's Acoustic Analogy is applied to investigate the noise radiated by a low Mach number flow through a ducted diaphragm. The simulation method is a two-step hybrid approach relying on Lighthill's acoustic analogy, assuming the decoupling of noise generation and propagation. The first step consists in an incompressible Large Eddy Simulation of the turbulent flow field, during which aerodynamic quantities are recorded. In the second step, a variational formulation of Lighthill's Acoustic Analogy using a finite element discretization is solved in the Fourier space. The sensitive steps consisting in computing and transferring source term data from the fluid mesh to the acoustic mesh are reviewed. Indeed, as fluid and acoustic meshes have different constraints due to the different wavelengths to be resolved, interpolation is required.

The method is applied to a three-dimensional ducted diaphragm with low Mach number flow. Although the configuration is symmetric, this study exhibits very complex three-dimensional developments. Aerodynamic results obtained from two different computing codes are compared with Direct Noise Computation performed by Gloerfelt & Lafon. Good agreement is found in terms of mean flow as well as on instantaneous behavior. Acoustic computations are performed with different mesh refinement and interpolation methods, showing their primary importance. Comparison with literature data on similar cases shows the method relevancy.

Introduction

In an industrial context, the development of an efficient hybrid noise computation method has to take into account its applicability and the computing time required to reach a relevant solution. In this work, two aerodynamic solutions obtained with different flow solvers are compared. The complete aeroacoustic process is explained: transfer of aerodynamic data from the CFD mesh to the acoustic mesh, source terms computation, application of filters to damp sources before they reach the acoustic domain boundaries, and resolution of the acoustic propagation problem. In particular, the interpolation of source terms onto the acoustic mesh is explained. Indeed, depending on the interpolation method chosen, the acoustic mesh in source regions may have to be refined to accurately represent source terms. This has a great impact on the computing time and resources necessary for the acoustic finite element simulation. After introducing the simulation method with theoretical developments, its practical implementation is explained, and the interpolation issue is discussed. The method is then applied to the case of a ducted diaphragm with a low Mach number flow, with comparisons between different flow solutions and interpolation methods. Finally, conclusions are drawn.

Simulation method

The simulation method is a two step hybrid approach relying on Lighthill's acoustic analogy [1], assuming the decoupling of noise generation and propagation. The first step consists of an incompressible Large Eddy Simulation of the turbulent flow field, during which aerodynamic quantities are transiently recorded. In the second step, a variational formulation of Lighthill's

Acoustic Analogy discretized by a finite element discretization is solved in the Fourier space, leading to the radiated noise up to the free field thanks to the use of infinite elements [2].

Theory

The implementation of Lighthill's acoustic analogy was firstly derived by Oberai et al [3]; refer also to Actran User's Guide [2] and Caro et al [4] for instance. The starting point is Lighthill's equation:

$$\frac{\partial^2}{\partial t^2}(\rho-\rho_0)-c_0^2\frac{\partial^2}{\partial x_i \partial x_j}(\rho-\rho_0)=\frac{\partial^2 T_{ij}}{\partial x_i \partial x_j} \tag{1}$$

with

$$T_{ij}=\rho u_i u_j+\delta_{ij}\left((p-p_0)-c_c^2(\rho-\rho_0)\right)-\tau_{ij} \tag{2}$$

Where ρ is the density and ρ_0 its reference value in a medium at rest, c_0 is the reference sound velocity, T_{ij} is Lighthill's tensor, u_i are the velocity components, p is the pressure and τ_{ij} is the viscous stress tensor. The variational formulation of Lighthill's analogy is then obtained after writing the strong variational statement associated with equation (1), and after integrating by parts along spatial derivatives following Green's theorem. This formulation is actually an equation on the acoustic density fluctuations $\rho_a = \rho - \rho_o$, which reads:

$$\int_\Omega\left(\frac{\partial^2\rho_a}{\partial t^2}\delta\rho+c_c^2\frac{\partial\rho_a}{\partial x_i}\frac{\partial\delta\rho}{\partial x_i}\right)d\mathbf{x}=-\int_\Omega\frac{\partial T_{ij}}{\partial x_j}\frac{\partial\delta\rho}{\partial x_i}d\mathbf{x}+\int_{\partial\Omega=\Gamma}\frac{\partial\Sigma_{ij}}{\partial x_j}n_i\delta\rho d\Gamma(\mathbf{x}) \tag{3}$$

where $\delta\rho$ is a test function, Ω designates the computational domain, and Σ_{ij} is defined as

$$\Sigma_{ij}=\rho u_i u_j+(p-p_0)\delta_{ij}-\tau_{ij} \tag{4}$$

Two source terms can be distinguished: a volume and a surface contribution. However, when surfaces are fixed, the latest vanishes. Therefore, only the volume source term is considered in this study.

Practical application of the method

The method consists in coupling a CFD code with a finite element acoustic software where the variational formulation of Lighthill's acoustic analogy is implemented. The main steps of a practical computation, provided that an unsteady solution of the flow field has already been obtained, are as follows:

1. flow field analysis allows to determine in which flow region(s) acoustic source terms will be considered; an acoustic mesh is built on the whole region of interest for acoustics, with possibly finer elements in source terms regions;

2. the time history of the source terms, or of aerodynamic quantities required to compute it, is stored on the CFD mesh during the CFD computation within the CFD code;

3. the source terms, usually computed on the CFD mesh for better accuracy, are interpolated on the coarser acoustic mesh;

4. the unsteady source terms are transformed from time to spectral domain;

5. the acoustic computation is performed with Actran/LA [2], taking into account the spectral volume source terms.

On the interpolation

In these five steps, the third one, namely the interpolation from the CFD mesh to the acoustic mesh, is of primary importance. Indeed, all the interest of this hybrid aeroacoustic method lies in the decoupling of the noise generation from its propagation. The decoupling makes it possible to adapt each computational step with respect to its efficiency. In particular, the requirements in terms of grid resolution are usually one order of magnitude more severe in the CFD than in the acoustic computation. This is due to the difference in size of acoustic and turbulent wavelengths. Therefore, in order to keep a light and tractable acoustic mesh, an efficient interpolation of source terms from the CFD mesh to the acoustic mesh has to be defined. In this work, two types of interpolation are applied. A classical 4th order Lagrange polynomial interpolation on a fine acoustic mesh is compared to a conservative interpolation on a coarse acoustics mesh. Conservative interpolation is actually an integration of source terms on the acoustic finite elements. Moreover, it will be shown that the order of finite elements plays an important role when performing integration on a coarse mesh.

The ducted diaphragm at low Mach number

Presentation

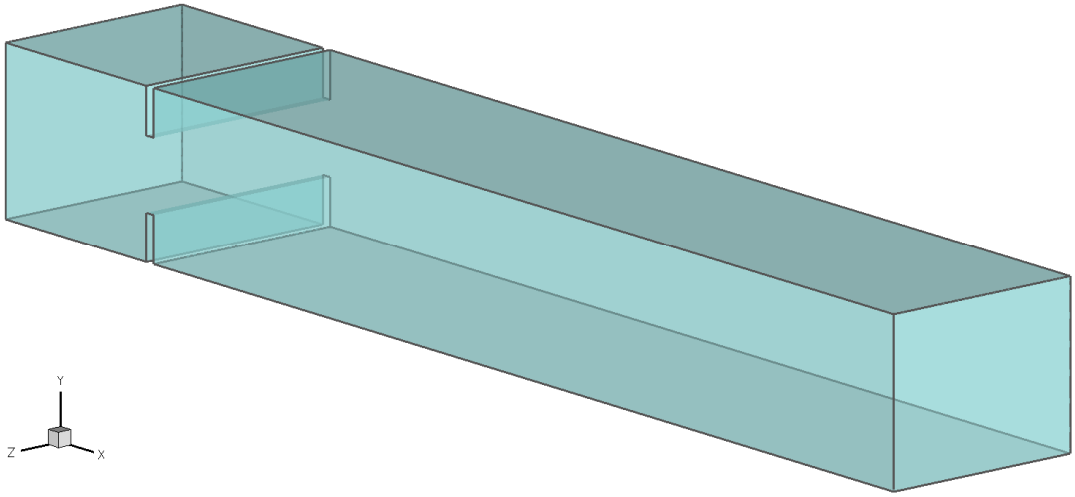

Figure 1: Diaphragm geometry. The x-axis indicates the streamwise flow direction; y- and z-axis respectively indicate the transverse and spanwise directions.

The case of the ducted diaphragm at low Mach number has been described extensively in Piellard et al [5][6]. It consists of a duct of rectangular cross-section obstructed by a diaphragm of height h, see Figure 1. This geometry is of particular interest since it represents an internal low velocity flow, for which few computational aeroacoustic studies are available.

In all simulations, the inflow velocity is fixed to 6m/s.

Flow field simulation

As already announced, different flow solutions are compared in this study. A brief aerodynamic comparison is proposed here.

Incompressible slice simulation

The first simulation, later denoted slice incompressible simulation, is performed on a slice of the domain consisting in 10% of the real width; a sketch of this reduced domain is given in Figure 2. A structured mesh of 843,000 cells is built, see Figure 2, where the finest cells in the area of the diaphragm and downstream of the diaphragm are of the order $h/70$. An incompressible Large Eddy Simulation is carried out with the finite volume code Fluent 6.3.26 [7] on this mesh.

Central differencing is used for the discretization of the momentum equation, PRESTO! for the pressure question, and the pressure-velocity coupling is taken into account via a PISO scheme. The time step satisfies a CFL number less or equal to unity for the smallest cell in the domain, yielding $\Delta t = 5.10^{-7}$s.

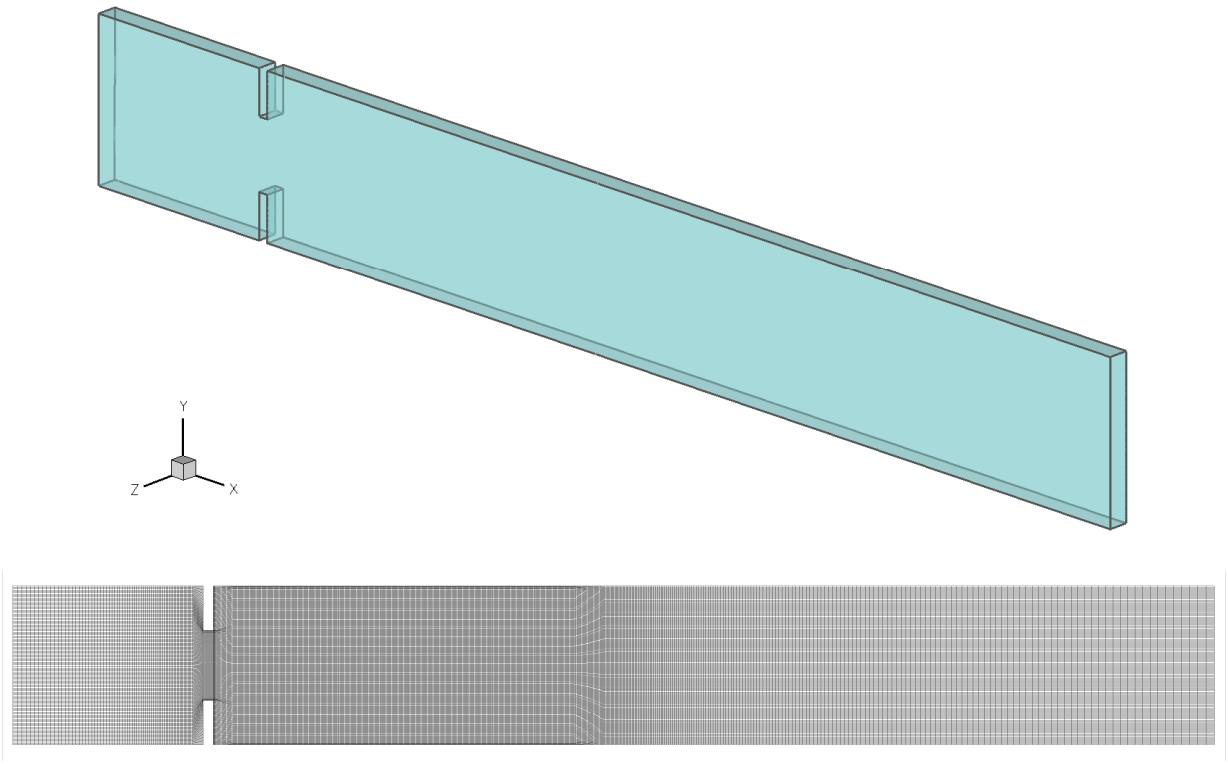

Figure 2: Diaphragm slice geometry and mesh.

Incompressible 3D simulation

In this second study, an incompressible Large Eddy Simulation is performed with Fluent [7] on the complete three-dimensional domain. The mesh, counting 8M cells, is very similar to the previous one, structured with finest cells downstream of the diaphragm of the order $h/70$. Discretization schemes are the same as for the incompressible slice simulation. The chosen time step $\Delta t = 10^{-5}$s corresponds to a maximum CFL number of 0.78.

Compressible 3D simulation

In this last study, the code Argo [8][9] developed at CENAERO has been used. Argo has a hybrid finite volume/finite element formulation, where convective terms are computed in a finite volume framework using linearly reconstructed face values (typically a Roe's approximate Riemann solver), and diffusive terms are computed using the Galerkin P1 finite element approximation. Full implicit time integration is performed using a second order 3-points Backward-Differencing scheme. For LES-type applications, Argo uses a second-order non-dissipative central scheme which conserves the kinetic energy at the discrete level. For industrial high-Reynolds number flow applications, a hybrid formulation based on the DES approach derived from the one-equation Spalart-Allmaras model is implemented. In order to achieve a discretization that is in accordance with the flow physics and the modeling strategy, the upwind scheme is used in the RANS region while the kinetic energy central scheme is active in the LES region.

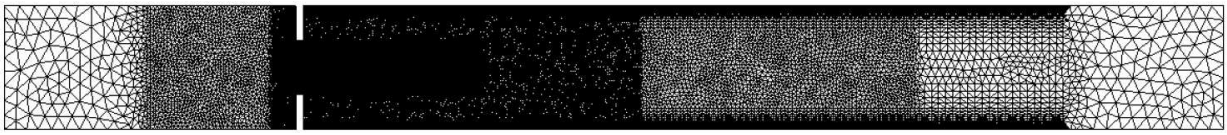

Figure 3: Mesh used for the compressible simulation.

An unstructured tetrahedral mesh is built on the same geometry as previously, slightly extended upstream and downstream, see Figure 3. The mesh is refined by blocks and counts a total of 5.6M nodes and 33.4M elements. Fine cells are found just downstream of the diaphragm, with a cell size of order $h/70$. Finer cells of size $h/140$ are locally placed around diaphragm edges, and a local near-wall refinement leads to the finest cell size of $h/3500$.

In this case, a RANS-LES simulation using Detached Eddy Simulation (DES) is chosen: RANS is applied near the walls if the local refinement is not enough for a pure « wall-resolved » LES, and LES is applied away from the walls and near walls if the mesh sufficiently refined. A low Reynolds correction of the DES model is activated as the Reynolds is moderate. The time step is $\Delta t = 5.10^{-5}$s.

Flow field results

Aerodynamic results of the incompressible slice simulation favorably compare to the LES simulation of Gloerfelt & Lafon [10], despite the truncation in the third direction. The main effect of the domain truncation is to constrain the flow to an exaggerated two-dimensional behavior. For the 3D incompressible and compressible simulations, almost no difference is noticed with reference [10] regarding aerodynamic results; the complex three-dimensional behavior of the flow for the incompressible simulation is described in [6]. Figure 4 presents the mean streamwise velocity fields for the three simulations, illustrating previous comments on the solutions quality.

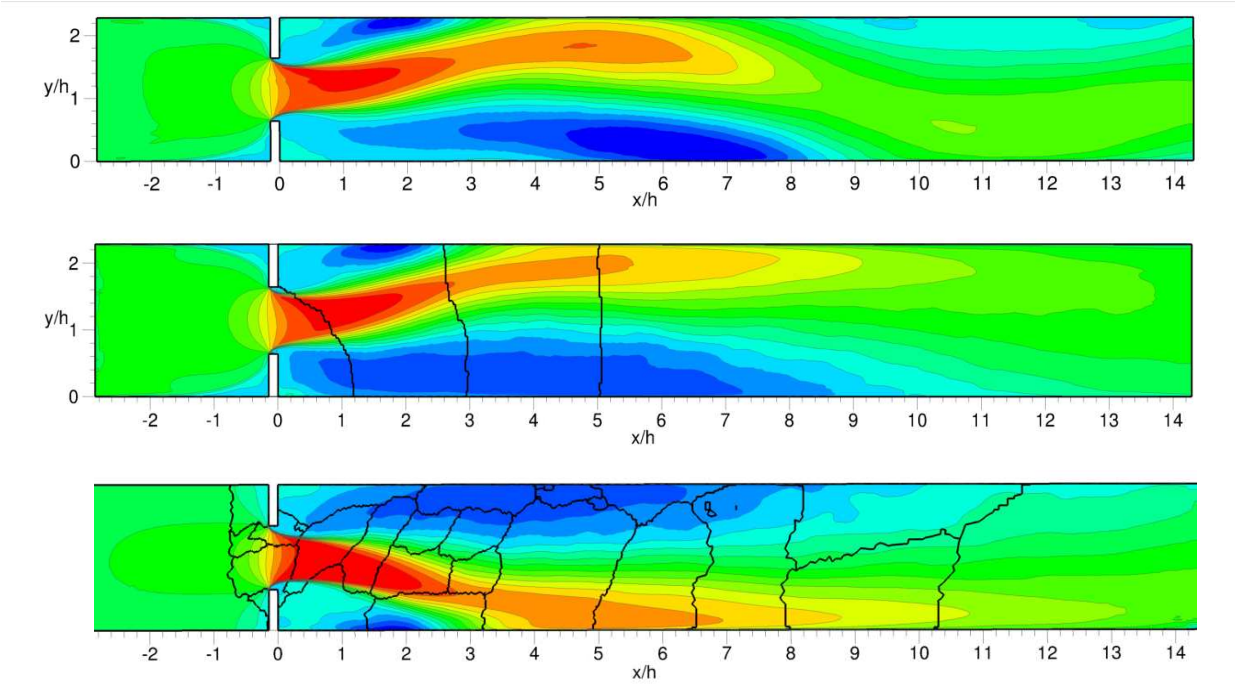

Figure 4: Mean streamwise velocity fields u/U_m for the three simulations, where the maximum mean velocity U_m=20m/s is used for normalization. Levels from -0.3 to 1. From top to bottom: incompressible slice, 3D incompressible, 3D compressible. Bold black lines indicate the location of partitions for parallel computations (8 partitions for the 3D incompressible simulation and 48 partitions for the 3D compressible simulation).

Acoustic simulations

Effect of the interpolation method

In order to study interpolation effects, three acoustic meshes are built and used with the data from incompressible simulations, with different interpolation methods.

A first two dimensional acoustic computation is performed, using the data recorded in the central XY plane of the incompressible slice CFD domain. The acoustic mesh is identical to the CFD mesh in the first part of the outlet duct and in the diaphragm region, and coarser elsewhere. The largest elements reach the mesh size of h=7, see Figure 5, allowing propagating the acoustic waves up to 10kHz. As the acoustic mesh is identical to the CFD mesh where source terms are computed, no interpolation is required to input the source terms in the acoustic computation; a basic mapping is simply performed. Source terms are defined only in the region of mesh refinement. Spatial filtering is also applied at the end of the source region to ensure a smooth transition to zero of the source terms toward the domain exit, see [5] for details.

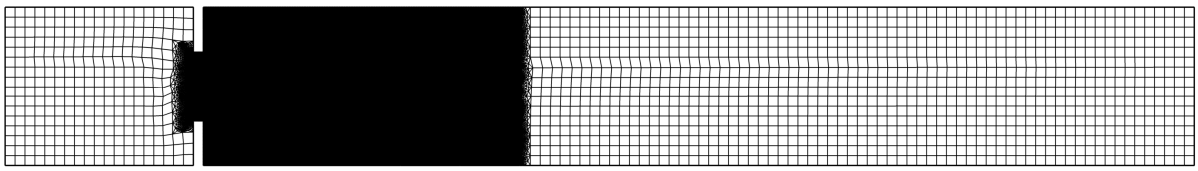

Figure 5: Diaphragm 2D acoustic mesh.

The second acoustic mesh is three-dimensional. It is extremely refined in the first part of the outlet duct, with the cell size equal to twice the CFD mesh size, see Figure 4. Because the acoustic mesh is not identical to the CFD mesh in source regions, interpolation is required to define acoustic source terms on the acoustic mesh. A non conservative 4th order Lagrange polynomial interpolation is performed. Source terms are defined only in the region of mesh refinement. Spatial filtering is applied in the second part of the outlet duct to ensure a smooth transition to zero of the source terms toward the domain exit.

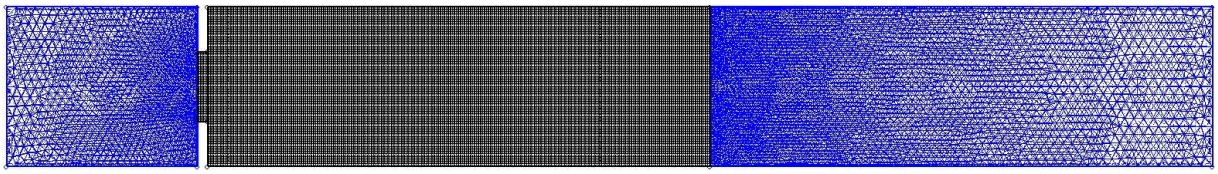

Figure 6: Diaphragm 3D refined acoustic mesh.

The last three dimensional acoustic mesh is built only with acoustic wave propagation requirements, without considering the presence or not of source terms. The mesh is uniform with a cell size of h=7 in the whole domain, see Figure 7. In this case, where interpolation is once more required, a new conservative interpolation scheme developed by Free Field Technologies [11] is applied. This interpolation actually consists in integrating source terms over the acoustic finite elements, preserving the energy contained in the source terms; more details about the integration definition can be found in [12]. For the corresponding acoustic computation, source terms are defined in the whole domain. Spatial filtering is applied in the second part of the outlet duct to ensure a smooth transition to zero of the source terms toward the domain exit.

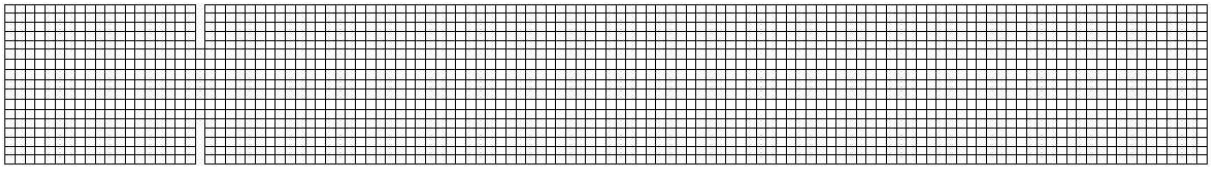

Figure 7: Diaphragm 3D coarse acoustic mesh.

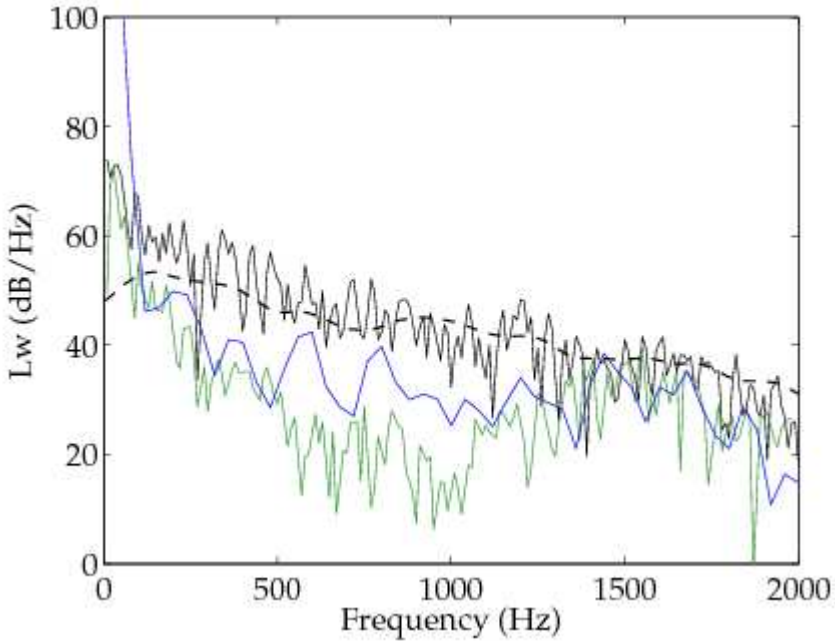

Figure 8: Acoustic power radiated at the end of the outlet duct. Dashed black line: reference results of Gloerfelt & Lafon [7]. Black: 2D computation without interpolation. Green: 3D computation with Lagrange interpolation. Blue: 3D computation with conservative interpolation, i.e. integration.

Acoustic results are given in terms of acoustic power radiated at the end of the outlet duct in Figure 8. It appears that, in spite of the limitations of the CFD slice computation, the corresponding two dimensional acoustic simulation, without interpolation, gives good results, with in particular the spectrum broadband shape similar to reference [10], over the whole frequency range [0-2000] Hz.

By contrast, three dimensional results on the fine acoustic mesh, with Lagrange polynomials interpolation, presents a broadband spectrum shape very different from the reference; a loss of energy in the frequency range [100-1400] Hz is particularly visible. This loss of energy is attributed to the information loss during interpolation, where roughly only 1/8th of the source terms information was kept, which corresponds to a decimation by 2 in each space direction from the CFD to the acoustic mesh.

Slightly better results are obtained with the coarse three dimensional acoustic mesh using integrated source terms. Note that in this last computation, only 50ms of signal was available, while 100ms were considered in previous simulations. The mandatory signal windowing (Hanning) has thus a great influence, and better results are expected with a longer simulation time.

Effect of the acoustic finite elements order

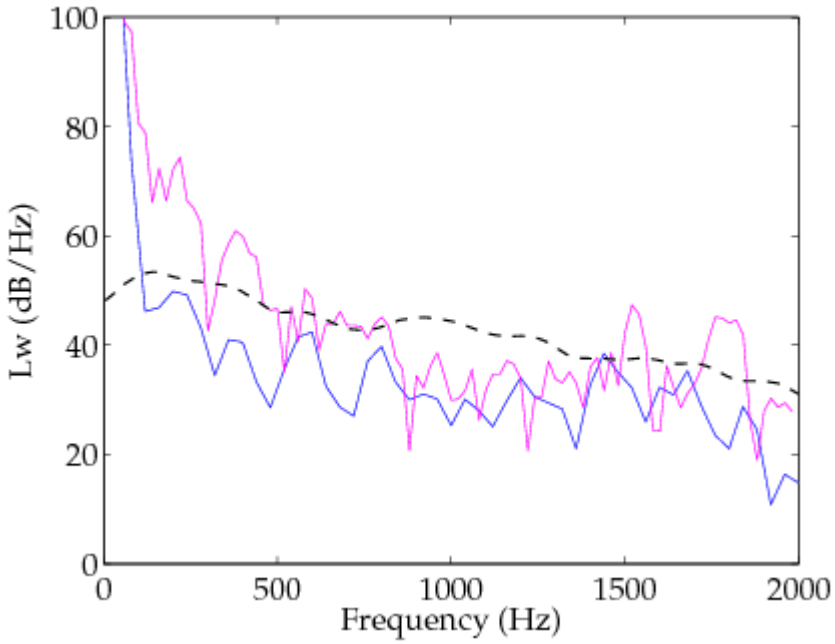

Figure 9: Acoustic power radiated at the end of the outlet duct. Dashed black line: reference results of Gloerfelt & Lafon [8]. Blue: 3D computation with conservative interpolation and linear finite elements. Magenta: 3D computation with conservative interpolation and quadratic finite elements.

In order to improve the results obtained with the incompressible CFD data integrated onto the coarse acoustic mesh, the order of acoustic finite elements is increased, and quadratic elements are used. Doing this roughly multiplies by a factor of 4 the number of integration nodes, in three dimensions. The computing time is also considerably increased, but as the Figure 9 attests it, the accuracy is also greatly increased. Indeed, source terms are now integrated on the finite elements taking intermediate points into account, which increases the fidelity of their representation. Very high levels are still present at low frequencies, and a slight hole is present in the range [800-1400]Hz.

Effect of the CFD resolution

A comparison of acoustic results obtained using the incompressible (Fluent) and compressible (Argo) CFD data is presented in Figure 10. The same coarse acoustic mesh described previously is used for all spectra, and source terms are obtained by integration. Results from the compressible code are very similar to the ones obtained with the incompressible LES and quadratic finite elements, which suggests that the refined CFD solution may improve acoustic results, even on a very coarse acoustic mesh. In particular, the finer CFD resolution of the compressible model in the diaphragm area may explain this improvement. In addition, results obtained with the compressible LES do not exhibit the unexplained peaks present in the other spectrum around 1500Hz and 1800Hz. In the low frequency range however, very high levels are still present. In both cases, i.e. incompressible and compressible LES data, better results are expected from the exploitation of longer signals, currently of 50ms and 29ms respectively.

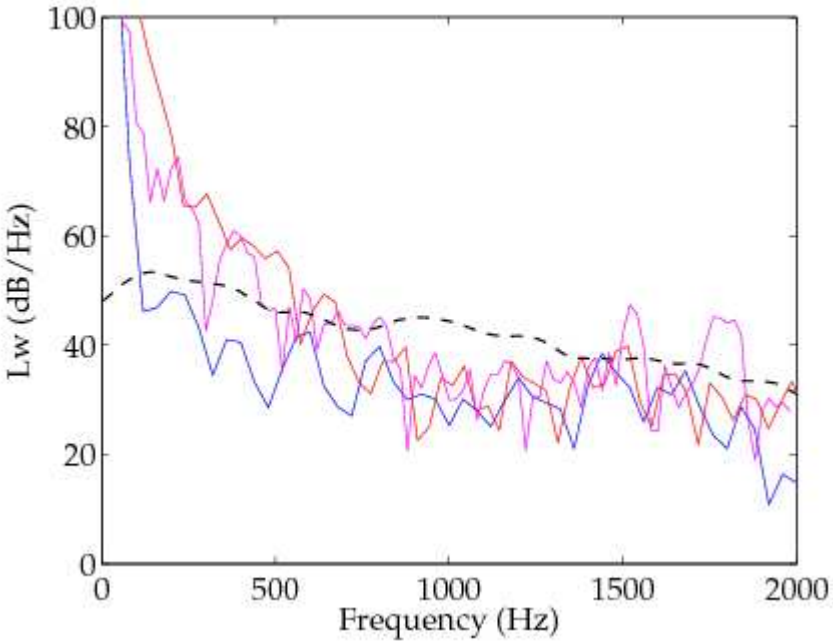

Figure 10: Acoustic power radiated at the end of the outlet duct. Dashed black line: reference results of Gloerfelt & Lafon [8]. Blue: 3D computation with conservative interpolation and linear finite elements. Magenta: 3D computation with conservative interpolation and quadratic finite elements. Red: 3D computation with conservative interpolation and linear finite elements using compressible CFD results from Argo.

Conclusions

In this work, the focus is put on the comparison of different strategies of source term interpolation from the CFD mesh to the acoustic mesh, and on the comparison of different CFD codes results. With no surprise, the best acoustic results are obtained when the CFD and the acoustic meshes are identical, requiring no interpolation at all for the source terms; this corresponds to the study on a slice of the domain. When interpolation is required, which is usually the case since an acoustic mesh as fine as the CFD mesh is not tractable in most applications, even a high order classical Cartesian interpolation is not sufficient to provide relevant results; the loss of information during non conservative interpolation cannot be retrieved by increasing the interpolation order. Besides, the use of a conservative interpolation, consisting of source terms integration, allows a more accurate representation of the source terms while preserving their energy. This last solution gives better results than classical interpolation. In addition, the comparison of previously obtained CFD data with results obtained by a different code and a different strategy is successful on the case of a ducted diaphragm at low Mach number flow. While CFD mesh and solvers are very different, mean as well as instantaneous aerodynamic quantities are similar. A more detailed aerodynamic comparison will be detailed in a future publication. Regarding acoustic spectra, the results are also very similar. Future investigations will allow studying the importance of signal length and of averaging.

Acknowledgements

The first author would like to greatly acknowledge CENAERO for providing CFD data obtained with their in-house code Argo.

References

[1] Lighthill, M.J., On sound generated aerodynamically. I: General theory. Proc. Roy. Soc. London A211, pp. 564-587, 1952.

[2] Free Field Technologies, Actran 2006 Aeroacoustic solutions, User's manual, 2006.

[3] Oberai, A.A., Ronaldkin, F., and Hughes, T.J.R., Computational procedures for determining structural-acoustic response due to hydrodynamic sources, Comput. Meth. in Applied Mech. and Eng., Vol. 190, 2000, pp. 345-361.

[4] Caro, S., Ploumhans, P., and Gallez, X., Implementation of Lighthill's Acoustic Analogy in a finite/infinite elements framework, AIAA Paper 2004-2891 , 2004.

[5] Piellard, M. and Bailly, C., Validation of a hybrid CAA method. Application to the case of a ducted diaphragm at low Mach number. AIAA Paper 2008-2873, 2008.

[6] Piellard, M., A hybrid method for Computational AeroAcoustics applied to confined geometries. PhD Thesis, Ecole Centrale de Lyon, 2008-25.

[7] Fluent Inc., Fluent 6.3 User's Guide, Sept. 2007.

[8] Georges, L., Winckelmans, G. S. and Geuzaine, P., Improving shock-free compressible RANS solvers for LES on unstructured meshes. Journal of Computational and Applied Mathematics, 215, pp. 419-428, 2008.

[9] Georges, L., Hillewaert, K., Capart, R., Thomas, J.-F., Louagie, T. and Geuzaine, P., RANS-LES simulations around a complete landing geometry. Proceedings of the 7th International ERCOFTAC Symposium on Engineering Turbulence Modelling and Measurements, 2008.

[10] Gloerfelt, X. and Lafon, P., Direct computation of the noise induced by a turbulent flow through a diaphragm in a duct at low Mach number. Computers & Fluids 37(4), 2008, pp. 388-401.

[11] Free Field Technologies, Actran/TM and Actran/LA 2009, User's guide, URL: www.fft.be, 2009.

[12] Caro, S., Detandt, Y., Manera, J., Toppinga, R., Mondonça, F., Validation of a new hybrid CAA strategy and application to the noise generated by a flap in a simplified HVAC duct. AIAA Paper 2009-3352.